Analyst

Accepted Manuscript

ROYAL SOCIETY OF CHEMISTRY

www.rsc.org/analyst

In this communication, we report that important protein remodeling processes, such as aggregation, unfolding and interaction with lipid membranes may be investigated by magnetic resonance imaging (MRI) through the chemical exchange saturation transfer (CEST) mechanism.

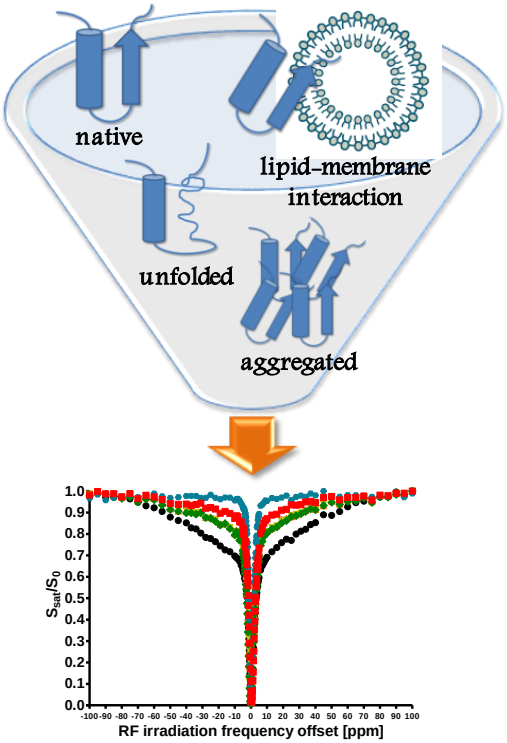

Analyst

RSCPublishing

COMMUNICATION

Chemical Exchange Saturation Transfer (CEST): an efficient tool for detecting molecular information on proteins' behaviour

Cite this: DOI: 10.1039/xoxxoooooox

Received ooth January 2012,
Accepted ooth January 2012

DOI: 10.1039/xoxxoooooox

www.rsc.org/

Dario Livio Longo,[ab*] Enza Di Gregorio,[a] Riccardo Abategiovanni,[a] Alberto Ceccon,[c] Michael Assfalg,[c] Henriette Molinari[c] and Silvio Aime[a]

A versatile method for assessing protein properties via magnetic resonance imaging (MRI) through chemical exchange saturation transfer (CEST) modality is described. The observed CEST signal changes allow to monitor protein aggregation processes, protein folding/unfolding steps and interaction with lipid membranes.

The advent of the MR cellular and molecular era has prompted the search for new paradigms in the design of MR imaging reporters. MRI-CEST agents are frequency-encoding probes.[1-4] They offer the possibility of designing novel experiments such as the multiplex detection in *in vivo* cell tracking or to map a specific physico-chemical parameter of the microenvironment in which they distribute.[5, 6] The CEST contrast arises from the decrease in the intensity of the bulk water signal following the saturation of the exchanging protons of the CEST agent by a selective radiofrequency (RF) pulse. Hence, the basic requisite for a CEST agent is that the exchange rate between its mobile protons and the bulk water protons has to be smaller than the difference between the absorption frequencies of the exchanging spins. In the CEST experiment, the RF pulse is applied at the absorption frequency of the exchanging protons to saturate their longitudinal magnetization. Because such nuclei exchange slowly with the nuclei of the bulk water, the intensity of the longitudinal magnetization of the latter will decrease from its equilibrium value.

The idea of transferring saturated magnetization to water proton resonance by irradiating the absorption of a proton pool of another molecule that is in a slow/intermediate exchange regime with water protons has been extensively exploited over the years in several fields of NMR spectroscopy. Its translation to MRI led to magnetization transfer contrast (MTC), which is the result of selectively observing the interaction of bulk water protons with the semi-solid macromolecular protons of a tissue. Differently from the semi-solid macromolecules, the absorption of the mobile protons of CEST molecules is generally relatively sharp and their frequencies precisely defined. The latter feature associates each CEST agent with its defined frequency-encoded property, thus opening the field to multiplex detection of different contrast agents in the same anatomical region.[7, 8] In recent years research in this field has progressed significantly and amide containing molecules have been extensively investigated as endogenous CEST agents. The procedure has been named Amide Proton Transfer (APT) and it has been shown to be able to report on early tumour detection, pH changes and response to therapy.[9-12] Moreover, amide/amine groups have been exploited for monitoring enzyme activity.[13, 14]

In principle the latter approach may be further extended to report about molecular transformations that occur at molecular level in tumour re-modeling processes. In fact either aggregation or de-aggregation of proteins intrinsically involves changes in the type, number and exchange rates of mobile protons as the structural changes invariantly modify the assets of the protein/water interface.

Proteins possess a variety of exchangeable proton pools, constituted by peptide amide groups and mobile side chain protons, including hydroxyl protons of threonine, serine and tyrosine, amino protons of lysine, amide protons of glutamine and asparagine, and guanidinium protons of arginine.[15] Moreover, solvent accessibility and hydrogen bonding strongly affect amide exchange rates, these being related to local and global protein stability.[16] The overall contribution to the saturation transfer effect of these mobile protons may therefore be investigated by a CEST experiment.

In Fig.1A the changes in the Saturation Transfer (ST) from exchangeable protons on Bovine Serum Albumin (BSA) was assessed upon a progressive heating of the protein-containing solution (5 mg/ml in PBS). The starting solution showed a broad ST effect from 0 to 5 ppm, peaking at ca. 2.5 ppm downfield from the water signal and originating mainly from exposed side chains and some of the solvent-exposed peptide bond amide protons of the protein (out of 582 total backbone H_N). Upon heating at 80 °C for 2, 5, 10, 30 and 60 min, the protein progressively aggregated passing from a neat solution to a semisolid white material. This change was accompanied by a progressive decrease of the level of ST in the CEST experiment due to formation of supramolecular aggregates, resulting in reduced chemical exchange rates and solvent accessibility. Moreover the ST curve appeared much flattened to indicate a largely increased line-width of protein signals upon formation of slow-tumbling supramolecular species.

Conversely, when the cross-linked BSA sample, obtained by the prolonged heating at 80 °C, was treated with a protease (Fig.1B), the resulting protein disaggregation process leads to a progressive increase of the ST level to reach a value of ca. 23% in the case of 4h treatment at 37 °C in presence of 150 µg enzyme/ml. Upon

representing the obtained results in the form of the so-called Z-spectra it becomes evident (Fig.1C) that the protein aggregation process leads to the formation of a large MT band (ca. 50 KHz wide), thus outlining an inverse relationship effect on the ST extent. These *in vitro* results exemplify *in vivo* processes involving protein reticulation (as in fibrosis processes), protein aggregations (such as the formation of amyloid plaques), or the activity of connective tissue-destroying enzymes (such as metallo-proteases in the extracellular tumour matrix), respectively.[17]

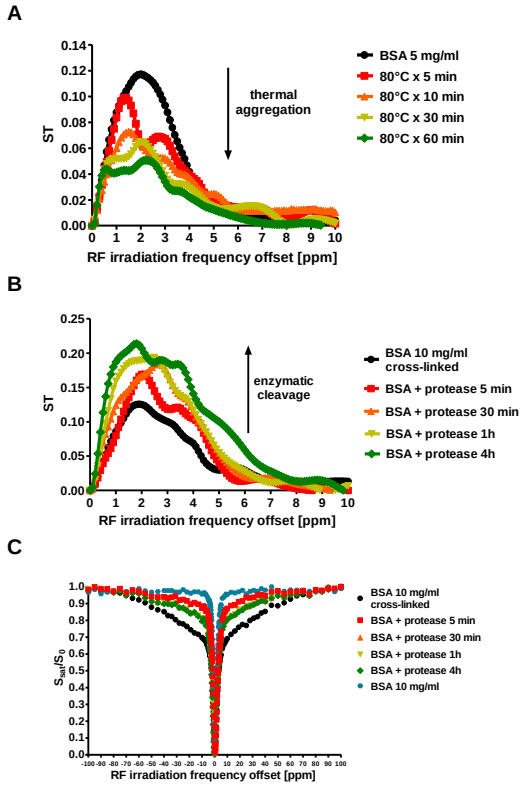

Figure 1. (A) Kinetics of thermal-induced BSA aggregation Saturation Transfer effect (ST) at 80 °C. (B) Study of the cleavage kinetics mediated by 150 µg/ml of protease on a cross-linked BSA sample (10 mg/ml). (C) Corresponding Z-spectra for the native BSA (10 mg/ml), the cross-linked BSA and the kinetics of protease cleavage.

Fundamental studies have clearly demonstrated the important role of modifications of the protein secondary structure in the aetiology of amyloidosis and related diseases.[18]

Protein unfolding normally occurs during physiological degradation of the macromolecule, but in some specific cases it is a consequence of genetic or environmental changes, resulting in the accumulation of aggregation-prone unfolded/misfolded proteins with attendant pathological outcomes.

To demonstrate the potential of the CEST approach to report about the unfolding processes in proteins, BSA and the human homologue, HSA, were titrated in phosphate buffer at pH 7.0 with the anionic surfactant sodium dodecyl sulphate (SDS). SDS is known to bind strongly to proteins and to induce their denaturation[19]The titration of BSA with increasing aliquots of SDS shows an initial slight increase of the ST effect at a molar ratio of 1:1, followed by a decrease for a ratio of BSA to SDS up to 1:4, and finally a steady increase of the ST curve with surfactant concentrations above 1 mM, which corresponds to ten SDS molecules per protein molecule (Figure 2A). The binding of SDS molecules to the protein induces conformational changes as well as exposure of several sidechains and backbone amides to the solvent, thus resulting in an increase of the number or of the chemical exchange rate of the mobile protons. Several models have been proposed for protein–SDS complexes. The most popular model for the SDS–BSA complex is the "pearl necklace" model in which the flexible denatured polypeptide chain of the protein has small spherical micelles clustered around it.[20] Therefore we can argue that an initial decrease of the ST curve may be associated to a conformational change, followed by several protein unfolding steps and polypeptide chain extension.

When the surfactant was added to HSA at identical concentration, we observed an initial decrease of the ST curve, followed by a continuous increase of the overall ST above 0.8 mM SDS concentration (Fig. 2C). In summary, for both proteins we observed an overall increase of the CEST effect upon protein denaturation, as expected by the unfolding of the protein and exposure of the buried secondary structure segments to solvent.

Fluorescence emission spectra of the intrinsic tryptophan (λ_{ex} = 295 nm) allow to monitor protein conformational changes upon surfactant binding. The tryptophan (Trp) fluorescence intensity generally decreases on exposure to a polar environment. For BSA (possessing two Trp residues, W^{131} and W^{214}) a similar trend in the fluorescence spectra was found compared to the CEST experiments: on addition of SDS we observed an initial increase in intensity, followed by a decrease with a blue shift and then a further increase in intensity and a further blue shift at higher surfactant concentrations (Fig. 2B). Instead, the titration of the HSA (possessing only one Trp, W^{214}) with SDS showed a steady enhancement of fluorescence up to 1 mM SDS concentration. The progressive blue shift of the maximum emission wavelength for both the BSA and HSA proteins is a typical behaviour observed in surfactant-induced protein unfolding.[21] Recently, a fluorescence study on the interaction of both BSA and HSA with SDS reported distinct spectroscopic changes for the two proteins, in agreement with the results obtained herein.[22] This spectroscopic difference may be explained by distinct effects of detergent molecules binding toW^{214} alone or to W^{214} and W^{131} local environments. Conversely, the MRI-CEST modality reports on effects on the overall proton pool, showing a similar progressive increase of the ST curves following the common unfolding process for both BSA and HSA upon surfactant-protein interaction.

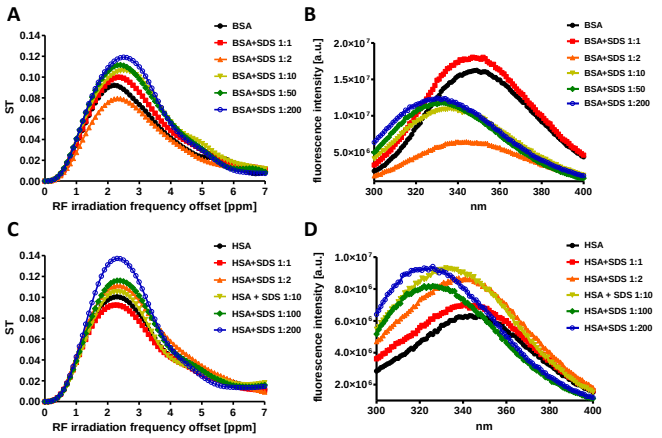

Figure 2. Saturation Transfer ST curves and fluorescence emission spectra of the intrinsic tryptophan of bovine serum albumin (A) and (B) and of human serum albumin (C) and (D), respectively, as a function of sodium dodecyl sulphate (SDS) concentrations in phosphate buffer at pH 7.0.

Similarly, a possible relationship between the CEST signal coming from the Nuclear Overhauser Effect (NOE) in the Z-spectrum and the structural state of the protein BSA has been investigated as a way to detect unfolding processes.[23]

Moreover the possibility of assessing changes in the CEST properties of a given protein may be relevant to gain insight into

microscopic details of its function. As an example we considered the interaction of BABP (Bile Acid Binding Protein) with the cellular membrane, an event that has been shown to be at the basis of the uptake of cholesterol metabolites into hepatocytes and their delivery to the biliary canaliculii[24-26]. The cellular membrane can be nicely mimicked by the outer surface of phospholipid vesicles (liposomes). In order to explore the role of electrostatics in the BABP-membrane interaction, liposomes displaying negative, neutral, or positive net charges were prepared (see caption to Fig.3). The ST shown by BABP (3.5 mg/ml in PF?) at 37° C is quite high (ca.23%) as expected by the relatively high number of exchangeable protons (a large solvent-accessible internal cavity is present). Upon addition of neutral or cationic liposomes (mean diameter of ca. 90 nm) no effect on the resulting CEST curve was detected. Conversely, a large decrease in the CEST effect was observed when the protein solution was presented with a negatively charged liposome of similar size (Fig. 3A).

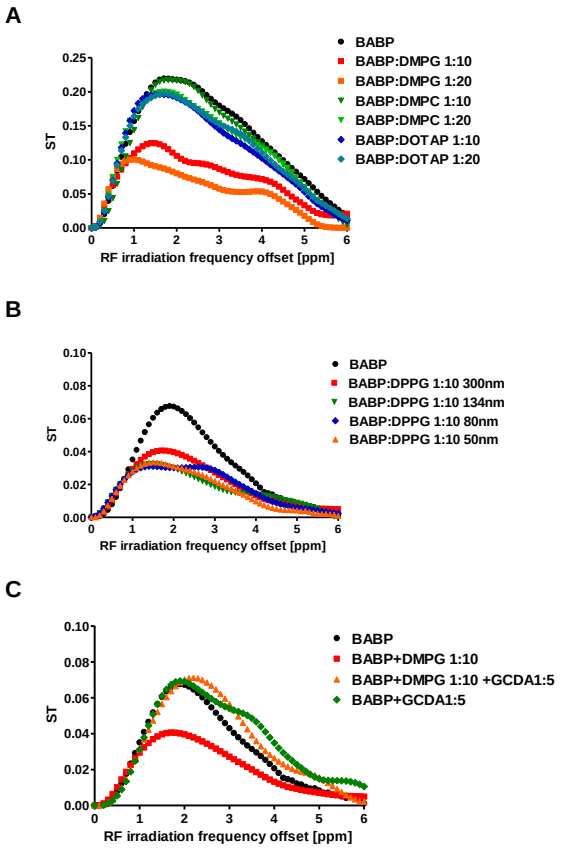

Figure 3 (A) Saturation transfer curves calculated from Z-spectra in the range 0–6 ppm for a 0.25 mM BABP solution (circles) and for BABP with anionic DMPG (squares), neutral DMPC (triangles) and cationic DOTAP (diamonds) liposomes at a lipid:protein molar ratio of 1:10 and 1:20. (B) Saturation transfer curves for a 0.1 mM BABP solution with anionic DPPG liposomes of different sizes ranging from 50 to 300 nm. (C) Saturation transfer curves for BABP 0.1 mM (circle), and in the presence of GCDA added to a ligand to protein ratio of 5, resulting in the formation of a protein–bile salt complex (diamonds), and, when DMPG-SUV were present with a protein:lipid ratio of 1:10 (squares), protein dissociation from the membrane was observed (triangles).

This is a clear indication that the interaction between BABP and the cellular membrane involves negatively charged domains of the latter and positively charged protein surface patches. The simple approach here proposed does not allow a deconvolution of all mechanisms contributing to the observed effect, which include "quenching" of chemical exchange at the protein-lipid interface and the progressive formation of supramolecular aggregates with the liposomes, resulting in removal of free BABP from solution. We note however that the 40% -50% reduction of ST in the range 0-5 ppm agrees well with the free protein fraction evaluated by NMR in similar ionic strength conditions.[27] Furthermore, the important achievement of this experiment is associated to the selectivity of the interaction that clearly indicates the strong interaction of the protein with negatively charged phospholipidic structures and demonstrates the collisional nature of the BABP-membrane interactions, an issue largely discussed in the literature.[28] The use of DMPG liposomes of different sizes, from 50 to 300 nm, demonstrated that the binding depends on a general property of the membrane, driven mainly by electrostatic interactions (Fig. 3B). We finally found that the measure of the CEST effect is able to assess the reversible binding of the protein to anionic vesicles. In fact, the addition of the ligand glycochenodeoxycholate to the BABP:DMPG 1:10 solution, caused the immediate release of the bound protein and the formation of the holo protein, evidenced by a recovery of the ST curve (Fig. 3C).[29] Moreover, the shape of the protein ST curves may reflect structural changes itself, with more dramatic or irreversible changes (e.g. thermal aggregation or enzymatic cleavage) followed by the loss of the bell-like shape (Fig. 1A), conversely less marked / reversible changes (e.g. conformational changes or protein interactions) proceeded keeping a similar bell-like shape (Fig. 2A).

Conclusions

In summary we demonstrated that the CEST modality developed for in vivo MRI may be efficiently applied *in vitro* to attain relevant information on the chemistry and functional properties of macromolecules by exploiting changes in prototropic exchange behaviour. The proposed approach may represent a new tool to investigate protein structure and behaviour, also complementing recently developed strategies to detect NMR-invisible molecular states.[30, 31]

This research was supported by grants from the Ministero dell' Istruzione, dell' Università e della Ricerca (grant numbers: RBFR08R7OU and 2009235JB7) and a grant from Cariverona Foundation (Verona Nanomedicine Initiative).

Notes and references

[a]Department of Molecular Biotechnologies and Health Sciences, University of Torino, 10126 Torino, Italy. E-mail: dario.longo@unito.it
[b]Institute for Biostructures and Bioimages (CNR) c/o Molecular Biotechnology Center, University of Torino, Via Nizza 52 10126 Torino, Italy
[c]Department of Biotechnology, University of Verona, 37134 Verona, Italy

†Electronic Supplementary Information (ESI) available: liposome preparation and characterization, UV-fluorescence and CEST experiments, additional CEST data. See DOI: 10.1039/c000000x/

1. E. Terreno, D. D. Castelli and S. Aime, *Contrast Media Mol Imaging*, 2010, **5**, 78-98.
2. P. C. van Zijl and N. N. Yadav, *Magn Reson Med*, 2011, **65**, 927-948.
3. E. Vinogradov, A. D. Sherry and R. E. Lenkinski, *J Magn Reson*, 2013, **229**, 155-172.
4. G. Liu, X. Song, K. W. Chan and M. T. McMahon, *NMR Biomed*, 2013, **26**, 810-828.
5. D. L. Longo, W. Dastru, G. Digilio, J. Keupp, S. Langereis, S. Lanzardo, S. Prestigio, O. Steinbach, E. Terreno, F. Uggeri and S. Aime, *Magn Reson Med*, 2011, **65**, 202-211.

6. D. L. Longo, A. Busato, S. Lanzardo, F. Antico and S. Aime, *Magn Reson Med*, 2012.
7. D. D. Castelli, E. Terreno, D. Longo and S. Aime, *NMR Biomed*, 2013, **26**, 839-849.
8. E. Terreno, W. Dastru, D. Delli Castelli, E. Gianolio, S. Geninatti Crich, D. Longo and S. Aime, *Curr Med Chem*, 2010, **17**, 3684-3700.
9. J. Zhou, B. Lal, D. A. Wilson, J. Laterra and P. C. van Zijl, *Magn Reson Med*, 2003, **50**, 1120-1126.
10. P. Z. Sun, J. Zhou, J. Huang and P. van Zijl, *Magn Reson Med*, 2007, **57**, 405-410.
11. D. Liu, J. Zhou, R. Xue, Z. Zuo, J. An and D. J. Wang, *Magn Reson Med*, 2012.
12. D. W. Klomp, A. N. Dula, L. R. Arlinghaus, M. Italiaander, R. D. Dortch, Z. Zu, J. M. Williams, D. F. Gochberg, P. R. Luijten, J. C. Gore, T. E. Yankeelov and S. A. Smith, *NMR Biomed*, 2013, **26**, 1271-1277.
13. D. V. Hingorani, E. A. Randtke and M. D. Pagel, *J Am Chem Soc*, 2013, **135**, 6396-6398.
14. G. Liu, Y. Liang, A. Bar-Shir, K. W. Chan, C. S. Galpoththawela, S. M. Bernard, T. Tse, N. N. Yadav, P. Walczak, M. T. McMahon, J. W. Bulte, P. C. van Zijl and A. A. Gilad, *J Am Chem Soc*, 2011, **133**, 16326-16329.
15. E. Liepinsh and G. Otting, *Magn Reson Med*, 1996, **35**, 30-42.
16. P. Weinkam, C. Zong and P. G. Wolynes, *Proc Natl Acad Sci U S A*, 2005, **102**, 12401-12406.
17. A. Aguzzi and T. O'Connor, *Nat Rev Drug Discov*, 2010, **9**, 237-248.
18. J. D. Sipe and A. S. Cohen, *J Struct Biol*, 2000, **130**, 88-98.
19. S. De, A. Girigoswami and S. Das, *J Colloid Interface Sci*, 2005, **285**, 562-573.
20. X. H. Guo, N. M. Zhao, S. H. Chen and J. Teixeira, *Biopolymers*, 1990, **29**, 335-346.
21. J. T. Vivian and P. R. Callis, *Biophys J*, 2001, **80**, 2093-2109.
22. E. L. Gelamo and M. Tabak, *Spectrochim Acta A Mol Biomol Spectrosc*, 2000, **56A**, 2255-2271.
23. M. Zaiss, P. Kunz, S. Goerke, A. Radbruch and P. Bachert, *NMR Biomed*, 2013, **26**, 1815-1822.
24. M. D'Onofrio, E. Gianolio, A. Ceccon, F. Arena, S. Zanzoni, D. Fushman, S. Aime, H. Molinari and M. Assfalg, *Chemistry*, 2012, **18**, 9919-9928.
25. M. D'Onofrio, L. Ragona, D. Fessas, M. Signorelli, R. Ugolini, M. Pedo, M. Assfalg and H. Molinari, *Arch Biochem Biophys*, 2009, **481**, 21-29.
26. M. Assfalg, E. Gianolio, S. Zanzoni, S. Tomaselli, V. L. Russo, C. Cabella, L. Ragona, S. Aime and H. Molinari, *J Med Chem*, 2007, **50**, 5257-5268.
27. A. Ceccon, M. D'Onofrio, S. Zanzoni, D. L. Longo, S. Aime, H. Molinari and M. Assfalg, *Proteins*, 2013, **81**, 1776-1791.
28. B. Corsico, H. L. Liou and J. Storch, *Biochemistry*, 2004, **43**, 3600-3607.
29. M. Pedo, F. Lohr, M. D'Onofrio, M. Assfalg, V. Dotsch and H. Molinari, *J Mol Biol*, 2009, **394**, 852-863.
30. N. L. Fawzi, J. Ying, R. Ghirlando, D. A. Torchia and G. M. Clore, *Nature*, 2011, **480**, 268-272.
31. P. Vallurupalli, G. Bouvignies and L. E. Kay, *J Am Chem Soc*, 2012, **134**, 8148-8161.